Theoretical "*t-z*" Curves for Piles in Radially Inhomogeneous Soil

Abigail H. Bateman[1] and Jamie J. Crispin[2]*

Abstract: Accurate estimates of pile settlement are key for efficient design of axially loaded piles. Calculations of pile settlement can be simplified using one-dimensional "*t-z*" curves describing pile settlement at a certain depth as a function of side friction. In the realm of this simplified framework, theoretical "*t-z*" curves can be derived by substituting an attenuation function describing the variation of shear stress with distance from the pile, into a soil constitutive model relating shear strain to shear stress, then integrating with respect to distance to get the settlement at the pile circumference due to an applied shear stress. A handful of analytical "*t-z*" curves are available in the literature using the concentric cylinder model to define an attenuation function; these include solutions for linear-elastic, power-law and hyperbolic constitutive models. However, radially homogeneous soil has often been assumed, ignoring the effect of the pile installation resulting in unconservative calculations of pile settlement. This paper considers the installation of the pile, resulting in a radially variable shear modulus distribution in the surrounding soil. A radial inhomogeneity correction factor has been developed for selected constitutive models based on two simplified functions for the soil inhomogeneity, which can be applied to the previously derived "*t-z*" curves produced assuming radially homogeneous soil. The performance of this simplified method is investigated.

Keywords: piles, settlement, "t-z" curves, radial inhomogeneity, soil/structure interaction

Introduction

Accurate estimation of pile settlement usually requires complex three-dimensional analysis, such as boundary element method solutions (e.g. Poulos and Davis, 1968; Butterfield and Banerjee, 1971; Poulos and Davis, 1980), finite element method solutions (e.g. Syngros, 2004, Ottaviani, 1975) and rigorous analytical solutions (Mylonakis, 2001, Anoyatis *et al*., 2019, Anoyatis and Mylonakis, 2020). However, even for the simplest case of a pile embedded in a homogeneous, linear-elastic half-space, they require complex numerical software. Simplified Winkler solutions are available (e.g. Mylonakis, 1995; Mylonakis and Gazetas, 1998; Guo, 2012; Scott, 1981 and Crispin *et al*., 2018) however these are limited to linear-elastic or linear-elastic, perfectly-plastic soil behaviour. Pile settlement calculations can instead be simplified using one-dimensional "*t-z*" curves (Seed and Reese, 1957; Coyle and Reese, 1966) that describe the relationship between the shear stress at the pile/soil interface and settlement experienced in an axially loaded pile at a specific depth. By discretising the pile and selecting a "*t-z*" curve for each section, a simple one-dimensional numerical analysis can be employed to calculate the settlement at the head of a pile due to an applied load.

While empirical "*t-z*" curves are available (e.g. Coyle and Reese, 1966; Vijayvergiya, 1977), they are limited to specific test configuration and are difficult to generalise to all pile dimensions, materials and installation methods as well as different site conditions. As an alternative, theoretical "*t-z*" curves can be derived analytically by substituting a soil shear stress attenuation function, $\tau(r)$, describing the radial attenuation of shear stress, into the flexibility form of a soil constitutive relationship, $\gamma(\tau)$ (Kraft *et al*., 1981; Anoyatis, 2009). The result, a function of strain in terms of radial distance, is integrated in the radial direction producing an Equation for the settlement experienced at the pile/soil interface due to the applied shear stress. This method was employed with the concentric cylinder model for radial attenuation of shear stress by Cooke (1974), Randolph and Wroth (1978) and Baguelin and Frank (1979) to derive a simple "*t-z*" relationship for piles embedded in linear-elastic soil. This solution has been extended to power-law (Vardanega *et al*., 2012) and hyperbolic (Kraft *et al*., 1981) constitutive relations for radially homogeneous soil.

Pile installation causes significant stress build-up in the surrounding soil, this results in reductions of soil strength and stiffness that are larger closer to the pile (O'Neill, 2001).

[1] Student, Department of Civil Engineering, University of Bristol, Bristol, UK

[2] Ph.D. Student, Department of Civil Engineering, University of Bristol, Bristol, UK

* Corresponding author, email: j.crispin@bristol.ac.uk

Experimental results using Spectral Analysis of Surface Waves (SASW) techniques were reported by Kalinski and Stokoe (1998) and Kalinski *et al.* (2001) which measured the variation of soil shear modulus with distance from a large open borehole in clay, confirming this behaviour. Therefore, in order to accurately model the installed pile response, the radial inhomogeneity of the surrounding soil must be considered. Kraft *et al.* (1981) modelled the effect of pile installation by utilising a linear shear modulus variation with distance from the pile. This was employed to derive an equivalent shear modulus, G_{ave}, for linear-elastic soil that can be substituted into the "*t-z*" curves for radially homogeneous soil to account for radial inhomogeneity.

Kraft *et al.* (1981) made two assumptions in the derivation of G_{ave}: the radial variation of shear modulus can be modelled with a simple linear function and an equivalent shear modulus can be selected based on a linear-elastic constitutive model, both with minimal loss of accuracy. This paper derives an inhomogeneity correction factor, similar to $G_{ave,}$ for linear-elastic and non-linear constitutive models based on a radial variation of shear modulus described using linear and power-law functions. These are used to investigate the validity of the assumptions made by Kraft *et al.* (1981).

Problem Definition

Figure 1 shows the deformation of a horizontal slice of soil due to an axial load on a circular pile of diameter, d. The displacement at the pile-soil interface, u_0, can be calculated by integrating the shear strain with respect to the radial distance from the pile, r. Assuming the radial deformations are negligible, this leads to Equation 1 (Randolph and Wroth, 1978):

$$u_0 = \int_{d/2}^{\infty} \gamma(r)\ dr \tag{1}$$

Two functions are required to refine the strain Equation: the attenuation function, $\tau(r)$, to describe the attenuation of shear stress with radial distance from the pile and a constitutive relation, $\gamma(\tau)$, to describe stress-strain behaviour within the soil.

The attenuation function can be obtained from the concentric cylinder model employed by Cooke (1974), Randolph and Wroth (1978) and Baguelin and Frank (1979). The soil is
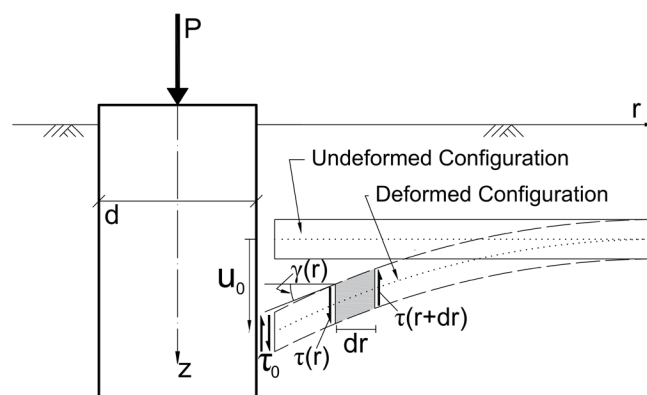

Figure 1. Deformation of a horizontal slice of soil due to an axial load on a pile

idealised as a series of concentric cylinders, the stresses on a small section of which is shown in Figure 2. Considering the vertical equilibrium of this soil element yields Equation 2:

$$\frac{\partial}{\partial r}(r\tau) + r\frac{\partial \sigma_z}{\partial z} = 0 \tag{2}$$

While rigorous solutions are available for this Equation (Mylonakis, 2001), a simplified solution can be obtained by assuming the variation with depth of the vertical normal stress, σ_z, is negligible (Randolph and Wroth, 1978; Scott, 1981). The second term is therefore ignored, and the first term integrated to give Equation 3 which describes the shear stress, τ, as a function of distance from the pile, r.

$$\tau(r) = \tau_0\left(\frac{d}{2r}\right) \tag{3}$$

where τ_0 is the shear stress at the pile/soil interface.

The constitutive relation must be in the flexibility form that gives shear strain, γ, in terms of the corresponding shear stress, τ. As a result of this, it is a requirement that a constitutive relationship in the form of $\tau(\gamma)$ must be analytically invertible. The simplest constitutive relationship is the linear-elastic stress-strain model:

$$\gamma = \frac{\tau}{G} \tag{4}$$

where G is the soil shear modulus.

Substituting Equation 3 into this relationship yields the shear strain as a function of distance from the pile, $\gamma(r)$. If this were inputted directly into Equation 1, infinite settlement would be predicted because the predicted settlement diverges as the radius from the pile considered increases. Instead, an empirical radius, r_m, is employed at which the settlement is assumed to be negligible. This results in Equation 5 (Randolph and Wroth, 1978, Fleming *et al.,* 2009):

$$\frac{u_0}{d} = \frac{\tau_0}{2G}\int_{d/2}^{r_m}\frac{1}{r}dr = \frac{\tau_0}{2G}ln\left(\frac{2r_m}{d}\right) \tag{5}$$

Randolph and Wroth (1978) assumed r_m to be proportional to the length of the pile, l, and $(1-v)$, where v is the Poisson's ratio of the soil. This has been written in general form by Mylonakis and Gazetas (1998), shown in Equation 6. The magnitude of settlement is approximately zero at 26 pile diameters, giving a suitable approximation of the product of the empirical constants, χ_1 and χ_2, to be about 2.5 for homogeneous, elastic half-space conditions (Randolph and Wroth, 1978, Mylonakis and Gazetas, 1998).

$$r_m \approx \chi_1\chi_2 l(1-v) \tag{6}$$

Equation 5 describes a linear-elastic "*t-z*" curve, this remains valid until slip occurs at the pile-soil interface. Figure 3(a) shows the full linear-elastic, perfectly-plastic constitutive model for London Clay where the shear stress is capped at a failure stress, $\tau_{max} = c_u$, the undrained shear strength. G was assumed to equal the initial shear modulus at small strain, G_0.
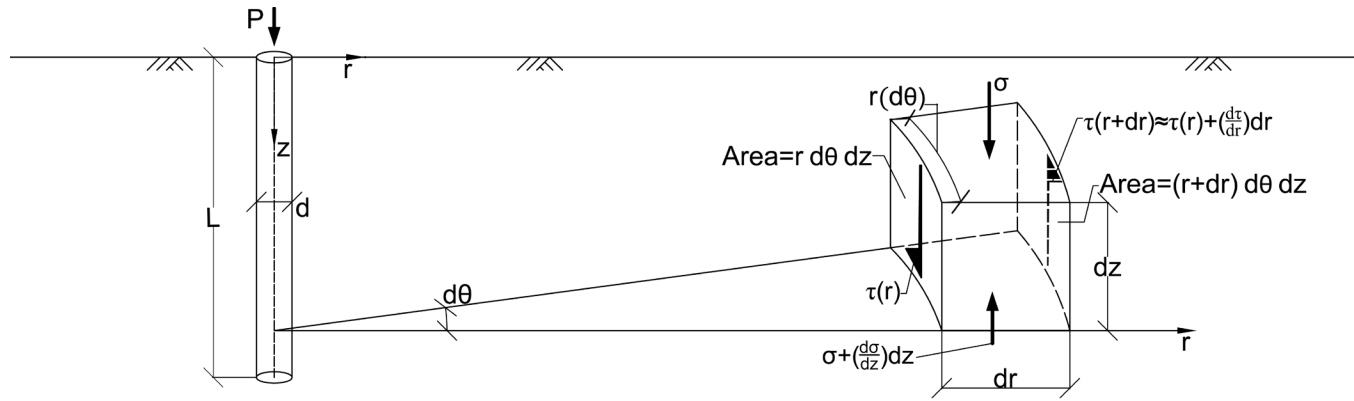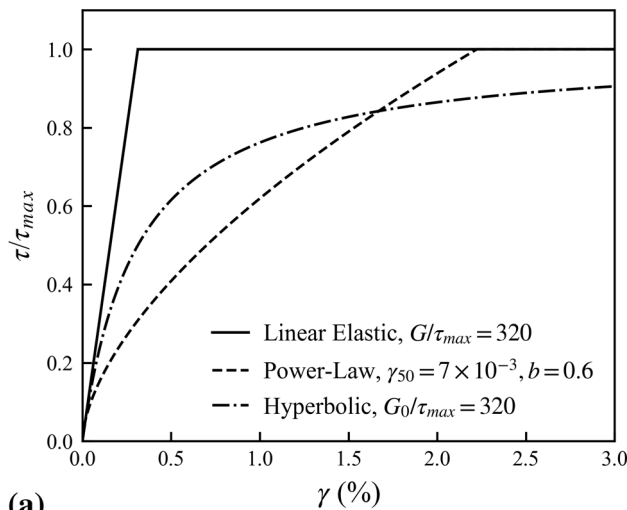
Figure 2. Derivation of the concentric cylinder model attenuation function
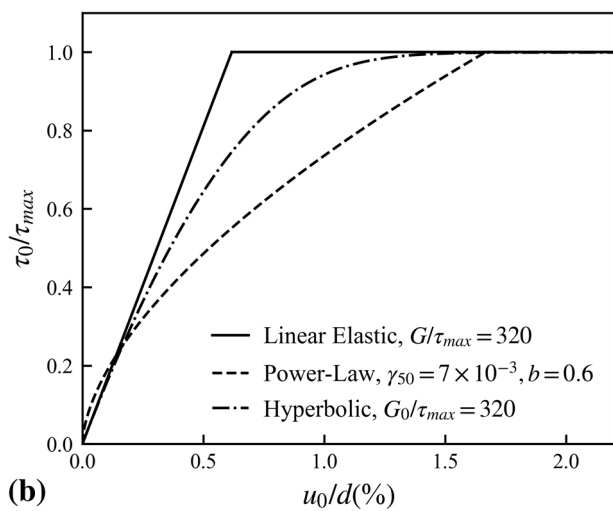
From a database of high quality triaxial tests in London Clay, Vardanega and Bolton (2011a) found that G_0/c_u in London Clay is approximately 320.

Figure 3(b) shows the "t-z" curve for linear-elastic soil using Equation 5 with $G=G_0$ and $\tau_{max}=c_u$. This is plotted up to

(a)

(b)

Figure 3. (a) London Clay modelled with different constitutive models (b) "t-z" curves for homogeneous soil, $r_m/d = 26$

τ_{max}, however, the strength of the pile/soil interface is normally less than the soil shear strength. In this case the "t-z" curve may be capped at a lower shear stress than τ_{max}. Skempton (1959) derived an empirical adhesion factor, α, on undrained shear strength, c_u, for this purpose which was based on a set of pile load tests in London Clay.

Radially Inhomogeneous Soil

The solution in Equation 5 assumes the soil shear modulus, G, is constant with distance from the pile; however, pile installation results in a softened zone being developed close to the pile. Kraft *et al.* (1981) suggests this can be modelled using a linear variation of shear modulus, $G(r)$, with distance from the pile/soil interface to the radius of influence of pile installation, r_i, (Figure 4(b)), which can be written as Equation 7 (Anoyatis, 2009).

$$G(r) = G_u \left[\left(\frac{G_d}{G_u} \right) + \left(1 - \frac{G_d}{G_u} \right) \left(\frac{r - d/2}{r_i - d/2} \right) \right], \ r \leq r_i \quad (7a)$$

$$G(r) = G_u, \ r > r_i \quad (7b)$$

where G_d is the disturbed shear modulus at the pile-soil interface and G_u undisturbed shear modulus prior to installation of the pile.

Employing a finite element method, Randolph *et al.* (1979) predicted that once consolidation of the soil is complete, a radius of around 10 pile diameters has altered stresses due to pile driving. Kraft *et al.* (1981) fitted Equation 7 through the data produced by Randolph *et al.* (1979) producing a value of radius of influence of pile installation, r_i, of approximately 7 pile diameters and a value for the reduction in the shear modulus at the pile/soil interface (G_d/G_u) of approximately 0.3.

The effects of the pile installation have been measured experimentally at a site at the University of Houston, Texas, by obtaining data using the Spectral Analysis of Surface Waves (SASW) at varying depths within a 3m (9.5ft) deep and 1m (3.5ft) diameter borehole, shown in Figure 4(a) (Kalinski, 1998). The test results are shown in Figure 4(b)

(O'Neill, 2001) and indicate the radius of influence of pile installation, r_i, is approximately 1 to 2 pile diameters away from the pile/soil interface and results in a disturbed shear modulus, at the pile/soil interface, G_d, of approximately half of the undisturbed value of shear modulus, G_u. Based on these results, O'Neill (2001) determined a "probable variation" of shear modulus with distance from the pile. Fitting Equation 7 to this probable variation gives r_i/d=1.75 and G_d/G_u=0.53, this is shown in Figure 4(b).

These results are empirical and are limited in application to bored piles in the over-consolidated (OCR>6) stiff clay at the Houston site (Kalinski *et al.*, 2001). The authors are not aware of any high-quality testing in other deposits or for other installation methods such as driven piles. However, the numerical results from Randolph *et al.* (1979) are for driven piles in Boston Blue Clay at a variety of OCR values. These indicate that driven piles have a much larger radius of influence, which is expected from the larger disturbance involved in their installation compared to bored piles. Additional numerical analysis and experimental results are required to allow the radial inhomogeneity parameters to be estimated with confidence in different soils and for different installation methods.
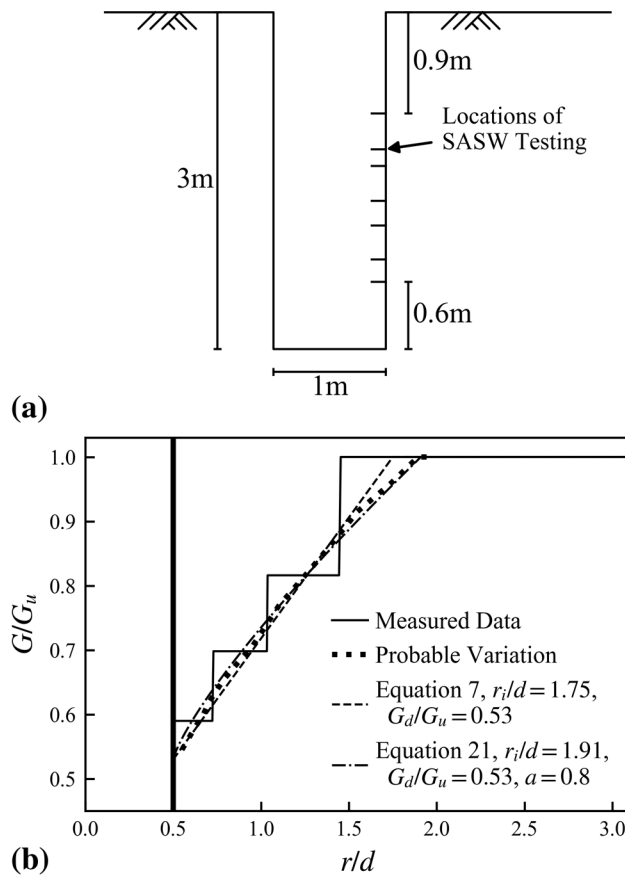

(a)

(b)

Figure 4. (a) Borehole dimensions and SASW testing locations (data from Kalinski 1998) (b) Variation of shear modulus with distance from the pile/soil interface (data from O'Neill, 2001, measured data attributed to Kalinksi and Stokoe, 1998)

Equation 7 can be substituted into the constitutive relation prior to the attenuation function in order to generate a "*t-z*" curve for radially inhomogeneous soil. In this case, Equation 1 can be rearranged to Equation 8.

$$u_0 = \int_{d/2}^{r_i} \gamma\left(r < r_i\right) dr + \int_{r_i}^{r_m} \gamma\left(r \geq r_i\right) dr \tag{8}$$

Employing the linear-elastic constitutive relation in Equation 4 and the attenuation function in Equation 3, the pile displacement for an applied shear stress is given by Equation 9.

$$\frac{u_0}{d} = \frac{\tau_0}{2G_u}\left[\frac{\frac{2r_i}{d}-1}{\frac{G_d}{G_u}\frac{2r_i}{d}-1} ln\left(\frac{G_d}{G_u}\frac{2r_i}{d}\right) + ln\left(\frac{r_m}{r_i}\right)\right] \tag{9}$$

Comparing this to Equation 5, replacing G with G_u, Equation 9 can be rearranged in the form:

$$\frac{u_0}{d} = \psi \frac{\tau_0}{2G_u} ln\left(\frac{2r_m}{d}\right) \tag{10}$$

where ψ is a radial inhomogeneity correction factor given by Equation 11. This is equivalent to G_u/G_{ave} in the notation of Kraft *et al.* (1981).

$$\psi = \left(\frac{\frac{2r_i}{d}-1}{\frac{G_d}{G_u}\frac{2r_i}{d}-1}\right) \frac{ln\left(\frac{G_d}{G_u}\frac{2r_i}{d}\right)}{ln\left(\frac{2 r_m}{d}\right)} + \frac{ln\left(\frac{r_m}{r_i}\right)}{ln\left(\frac{2 r_m}{d}\right)} \tag{11}$$

Non-Linear Soil Behaviour

Kraft *et al.* (1981) suggest that a radial inhomogeneity correction factor developed using a linear-elastic soil is suitable to model installation effects and that general nonlinear effects are more important to consider than the effect of soil nonlinearity on the installation effect. Two simplified nonlinear soil models are employed here to investigate this assumption, a power law model (Vardanega *et al.*, 2012) and a hyperbolic model (Konder, 1963).

Vardanega *et al.* (2012) used the power-law constitutive relationship in Equation 12 to develop a "*t-z*" curve incorporating non-linear soil behaviour.

$$\frac{\tau}{c_u} = \frac{1}{2}\left(\frac{\gamma}{\gamma_{50}}\right)^b \tag{12}$$

where γ_{50} is the shear strain during the mobilisation of half the undrained shear strength, c_u is the undrained shear strength, τ is the mobilised shear stress and b is a soil nonlinearity exponent. This constitutive model, calibrated for the stress range shown by Vardanega and Bolton (2011b) using a database of soil tests in clays and silts, is shown in Figure 3(a). Vardanega and Bolton (2011a) found the average γ_{50} for London Clay is

0.007. Vardanega and Bolton (2011b) derived a mean value of $b=0.60$ with standard deviation 0.15. Rearranging Equation 12 into the flexibility form with γ as the subject and substituting in Equation 3, the power-law relationship defining shear strain as a function of radial distance is obtained. This can be integrated using Equation 1, noting r_m does not need to be applied. This results in Equation 13 (Vardanega *et al.*, 2012, Vardanega, 2015, Crispin *et al.*, 2019) which is shown in Figure 3(b).

$$\frac{u_0}{d} = \frac{b\gamma_{50}}{2(1-b)}\left(\frac{2\tau_0}{\tau_{max}}\right)^{\frac{1}{b}} , \ b < 1 \tag{13}$$

Similarly to the linear-elastic constitutive model, a radial inhomogeneity correction factor, ψ, can be defined to allow pile installation effects to be considered, shown in Equation 14.

$$\frac{u_0}{d} = \psi \frac{b\ \gamma_{50}}{2(1-b)}\left(\frac{2\tau_0}{\tau_{max}}\right)^{\frac{1}{b}} , \ b < 1 \tag{14}$$

The inhomogeneity correction factor can then be calculated rigorously by substituting Equation 7 into the constitutive model in Equation 12, producing Equation 15:

$$\psi = \left(\frac{2\ r_i}{d}\right)^{\frac{b-1}{b}} - \left[\frac{\dfrac{2\ r_i}{d}-1}{\dfrac{G_d}{G_u}\dfrac{2r_i}{d}-1}\right]\left[\left(\frac{2\ r_i}{d}\right)^{\frac{b-1}{b}} g\left(\frac{2\ r_i}{d}\right)-g\left(1\right)\right] \tag{15a}$$

where $g(\ )$ is Gauss's Hypergeometric Function (Abramowitz and Stegun, 1972) with the following arguments:

$$g(x) =\ _2F_1\left(1,1-\frac{1}{b};2-\frac{1}{b};x\frac{\dfrac{G_d}{G_u}-1}{\dfrac{G_d}{G_u}\dfrac{2r_i}{d}-1}\right) \tag{15b}$$

Equation 15b is nontrivial to compute. Therefore, the recommendations by Kraft *et al.* (1981) to employ an inhomogeneity correction factor based on a linear-elastic constitutive model are appealing. This is investigated in Figure 5 where the "t-z" curves developed using Equation 14 and three different assumptions for ψ are compared: Equation 15 developed for non-linear soil, Equation 11 developed for linear-elastic soil and $\psi=1$ representing neglecting radial inhomogeneity completely and using the undisturbed soil parameters.

Figure 5(a) illustrates, that for $b=0.60$ the percentage difference between the two "t-z" curves is approximately 1%. Figure 5(b) shows this difference for a range of b values. Within the range $\pm1\sigma$ from the average b determined by Vardanega and Bolton (2011b) ($0.45 < b < 0.75$) the error is below 10%. This can be compared with the error when $\psi=1$, which is 23% at $b=0.6$, but increases to 31% within the
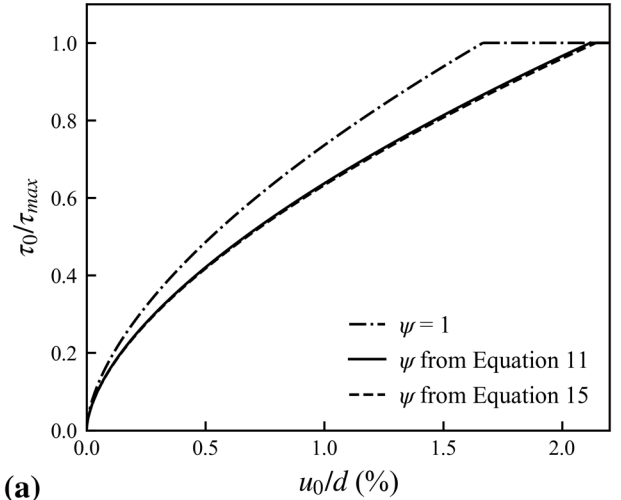
(a)
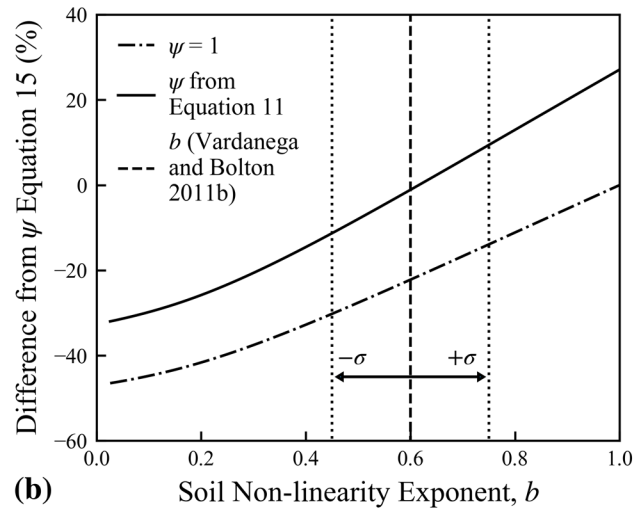
(b)

Figure 5. (a) Power-law "t-z" curve (Equation 14), $\gamma_{50} = 7 \times 10^{-3}$, $b = 0.6$ (b) Percentage difference between the "t-z" curves for varying soil non-linearity exponent values, $G_d/G_u = 0.53$, $r_i/d = 1.75$, $r_m/d = 3.86$

range $\pm1\sigma$. This indicates that radial inhomogeneity can be adequately accounted for using the simplified result in Equation 11 instead of Equation 15.

Kraft *et al.* (1981) developed a "t-z" curve using a hyperbolic constitutive model in the form of Equation 16:

$$G_{sec} = G_0\left[1-\left(\frac{\tau R_f}{\tau_{max}}\right)\right] \tag{16}$$

where G_0 is the initial shear modulus at small strain, G_{sec} is the secant shear modulus and R_f is a fitting constant. Different forms of this hyperbolic relationship have previously been analysed by Konder (1963) as a suitable stress-strain relationship. A similar hyperbolic model can be written in flexibility form as Equation 17. This is plotted in Figure 3(a).

$$\gamma = \frac{\tau}{G_0 - \dfrac{\tau G_0}{\tau_{max}}} \tag{17}$$

The "*t-z*" curve Equation using the concentric cylinder model (Equation 3) for radially homogeneous soil is shown in Equation 18 (Kraft *et al.*, 1981) and plotted for radially homogeneous soil in Figure 3(b).

$$\frac{u_0}{d} = \left(\frac{\tau_0}{2G_0}\right) ln\left(\frac{2\tau_{max} r_m - \tau_0 d}{\tau_{max} d - \tau_0 d}\right) \tag{18}$$

As before, a radial inhomogeneity correction factor, ψ, can be defined to allow pile installation effects to be considered, shown in Equation 19.

$$\frac{u_0}{d} = \psi\left(\frac{\tau_0}{2G_0}\right) ln\left(\frac{2\tau_{max} r_m - \tau_0 d}{\tau_{max} d - \tau_0 d}\right) \tag{19}$$

The inhomogeneous correction factor calculated for the hyperbolic constitutive model is given by Equation 20.

$$\psi = \frac{ln\left(\frac{2\tau_{max} r_m - \tau_0 d}{2\tau_{max} r_i - \tau_0 d}\right) + \dfrac{\left(\frac{2r_i}{d} - 1\right) ln\left(\frac{G_d}{G_u}\frac{2\tau_{max} r_i - \tau_0 d}{\tau_{max} d - \tau_0 d}\right)}{\frac{\tau_0}{\tau_{max}}\left(1 - \frac{G_d}{G_u}\right) + \left(\frac{2r_i}{d}\frac{G_d}{G_u} - 1\right)}}{ln\left(\frac{2\tau_{max} r_m - \tau_0 d}{\tau_{max} d - \tau_0 d}\right)} \tag{20}$$

Figure 6(a) illustrates the difference between the "*t-z*" curves produced from the linear-elastic constitutive model ψ, the hyperbolic constitutive model ψ and when $\psi=1$. Figure 6(b) quantifies this difference between the "*t-z*" curves as a result of the shear stress at the pile/soil interface. The percentage error in the "*t-z*" curve increases with the shear stress at the pile/soil interface, up to a (τ_0/τ_{max}) value of 0.85, the "*t-z*" curve using ψ from Equation 11 is within 10% of the curve using ψ from Equation 20. This is comparable to errors greater than 22% for $\psi=1$ when installation effects aren't considered. This is in agreement with the results shown in Figure 5, indicating the simplified ψ from Equation 11 is suitable for predicting response in radially inhomogeneous soil.
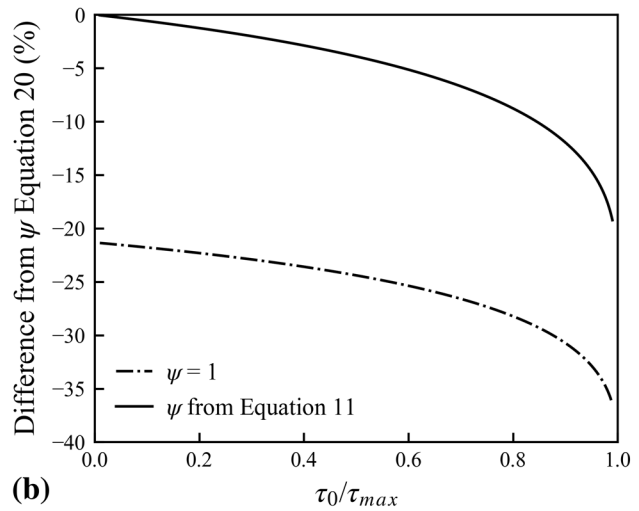
Non-Linear Radial Inhomogeneity

Due to the uncertainty in the actual radial variation in shear modulus due to pile installation, Kraft *et al.* (1981) assumed that the linear function in Equation 7 is adequate. The high-quality experimental data reported in Kalinski and Stokoe (1998) and Kalinski *et al.* (2001) allows this assumption to be investigated. An improved Equation to fit the variation in shear modulus with distance from the pile utilising a power-law function is shown in Equation 21:

$$G(r) = G_u\left[\frac{G_d}{G_u} + \left(1 - \frac{G_d}{G_u}\right)\left(\frac{r - d/2}{r_i - d/2}\right)^a\right], \; r \leq r_i \tag{21a}$$

$$G(r) = G_u, \; r > r_i \tag{21b}$$
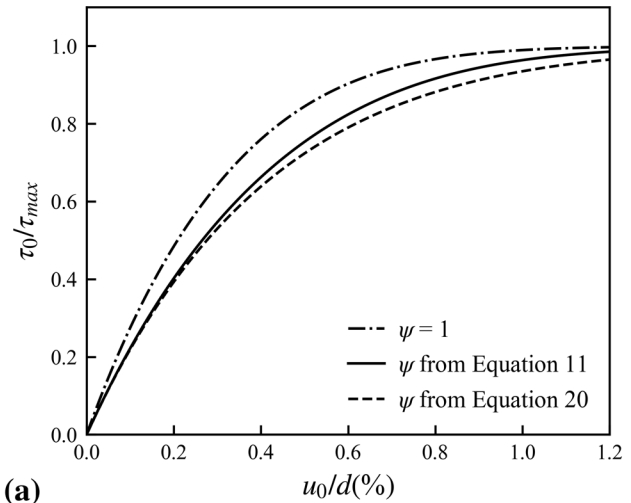
(a)

(b)

Figure 6. (a) Hyperbolic "*t-z*" curve (Equation 19), G_d/τ_{max} = 320 (b) Percentage difference between the "*t-z*" curves for varying shear stress at the pile/soil interface, G_d/G_u = 0.53, r_i/d = 1.75, r_m/d = 3.86

where *a* is a radial inhomogeneity exponent. Setting *a=1*, Equation 21 simplifies to Equation 7. Fitting Equation 21 to the probable variation provided in O'Neill (2001) gives a value of *a=0.8* and $r_i/d=1.91$.

An inhomogeneity correction factor, defined in Equation 10, can also be calculated for the linear-elastic constitutive model "*t-z*" curve and the power-law radial shear modulus variation, given by Equation 22. This cannot be analytically integrated; however, it can be calculated numerically.

$$\psi = \frac{\int_{\frac{d}{2}}^{r_i}\frac{1}{r}\left[\frac{G_d}{G_u} + \left(1 - \frac{G_d}{G_u}\right)\left(\frac{r - \frac{d}{2}}{r_i - \frac{d}{2}}\right)^a\right]^{-1} dr + ln\left(\frac{r_m}{r_i}\right)}{ln\left(\frac{2r_m}{d}\right)} \tag{22}$$

Figure 7 is used to validate the assumption in Kraft *et al.* (1981) by comparing the "*t-z*" curves produced from assum-
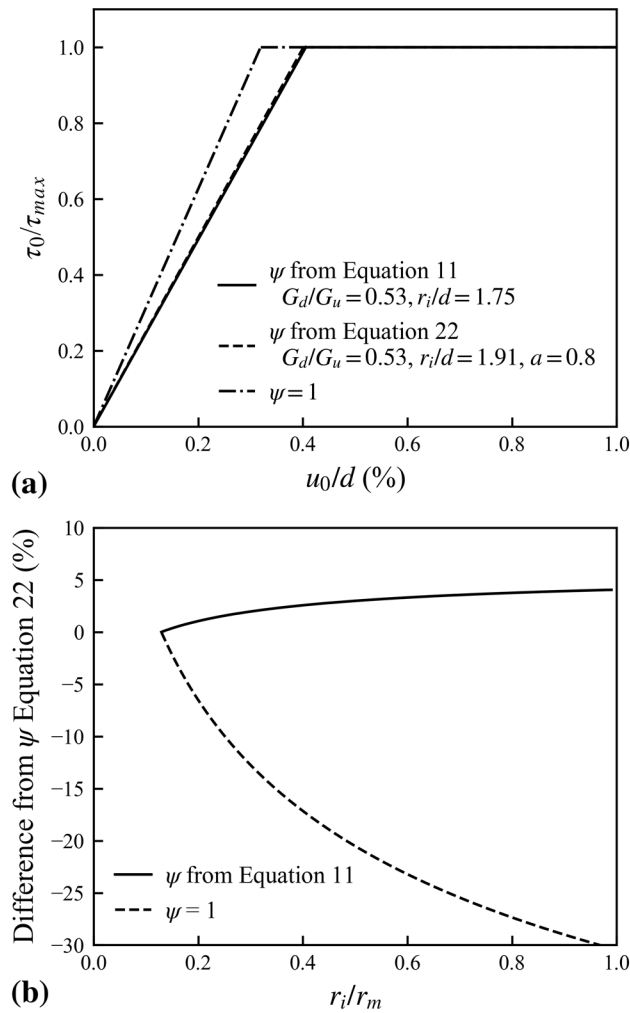
10/10/20   12:17 PM

Figure 7. (a) Linear "*t-z*" curve, $r_m/d = 3.9$ (b) Percentage difference between the "*t-z*" curves, $G_d/G_u = 0.53$, $a = 0.8$, $r_m/d = 3.9$

ing ψ values from: Equation 22 developed for a non-linear shear modulus variation, Equation 11 developed for linear-elastic soil and $\psi=1$ for radially homogeneous soil with the undisturbed shear modulus. Figure 7(a) shows that the "*t-z*" curve produced using ψ from Equation 11 overestimates settlement by approximately 2%. Ignoring pile installation effects and setting $\psi=1$ gives an error of 20% for the test configuration shown in Figure 4(a). The difference can be plotted against, r_i/r_m, which is shown in Figure 7(b). It is evident that the numerical integration required to calculate Equation 22 can be replaced with the simplified solution in Equation 11 without significant loss of accuracy.

Conclusion

Theoretical "*t-z*" curves can be derived by substituting an attenuation function describing the variation of shear stress with distance from the pile, into a soil constitutive model relating shear strain to shear stress, then integrating with respect to distance to get the settlement at the pile circumference due to an applied shear stress. A radial inhomogeneity correction factor, ψ, that can be applied to a "*t-z*" curve has been introduced

allowing pile installation effects to be modelled simply with only two radial inhomogeneity parameters required. However, limited data is available to calibrate these parameters. The method has been demonstrated using SASW data from a large borehole at a site in Houston, TX (Kalinski and Stokoe, 1998; Kalinski *et al.,* 2001), but the response in other soils and due to different installation methods requires further investigation.

ψ values were derived for the following cases:

- linear-elastic soil with a linear shear modulus variation with radial distance (Equation 11), matching previous work by Kraft *et al.* (1981);
- power-law (Equation 15) and hyperbolic (Equation 20) non-linear soil constitutive models with a linear shear modulus variation with radial distance;
- linear-elastic soil with a power-law shear modulus variation with radial distance (Equation 22), however this value must be approximated numerically.

The equivalent shear modulus calculated for the linear-elastic soil with the linear shear modulus variation (Equation 11) has been shown to be suitable for estimating the effects of the installation of the pile with minor error compared to the more rigorous solutions that are more complex to compute.

Acknowledgements

References

Abramowitz, M. and Stegun, I.A. (1972). Handbook of Mathematical Functions with Formulas, Graphs and Mathematical Tables. 10th Printing, 1st Edition. Applied mathematics series 55. National Bureau of Standards, USA.

Anoyatis, G. (2009) Elastodynamic analysis of piles for inertial and kinematic loading. MSc Thesis, School of Engineering, Civil Engineering Department, University of Patras, Rio, Greece. (in Greek).

Anoyatis, G., Mylonakis, G. and Tsikas, A. (2019). An analytical continuum model for axially loaded end-bearing piles in inhomogeneous soil. *International Journal for Numerical and Analytical Methods in Geomechanics*. https://doi.org/10.1002/nag.2886.

Anoyatis, G. and Mylonakis, G. (2020) Analytical solution for axially loaded piles in two-layer soil. *Journal of Engineering Mechanics*, ASCE. 146(3):04020003.

Baguelin, F. and Frank, R. (1979). Theoretical studies of piles using the finite element method. *Numerical Methods in Offshore Piling*. Institution of Civil Engineers, London: 83-91.

Butterfield, R. and Banerjee, P.K. (1971). The elastic analysis of compressible piles and pile groups. *Géotechnique*, 21(1): 43-60. DOI: 10.1680/geot.1971.21.1.43.

Cooke, R.W. (1974). The settlement of friction pile foundations. *Proceedings of the Conference on Tall Buildings*, Kuala Lumpur. CP 12/75.

Coyle, H.M. and Reese, L.C. (1966). Load transfer for axially loaded piles in clay. Journal of the Soil Mechanics and Foundations Division, *ASCE* 92(2): 1-26.

Crispin, J.J., Leahy, C.P. and Mylonakis, G. (2018). Winkler, model for axially loaded piles in inhomogeneous soil. *Géotechnique Letters* 8(4): 290-297.

Crispin, J.J., Vardanega, P.J., Mylonakis, G. (2019). Prediction of pile settlement using simplified models. *Proceedings XVII ECSMGE-2019*, Reyjavik, Iceland, September 1-6, 2019.

Fleming, K., Weltman, A., Randolph, M., and Elson, K. (2009). Piling engineering, 3rd edition. Taylor & Francis. Abdingdon, UK, 398 p.

Guo, W.D. (2012). Theory and practice of pile foundations, 1st edition, CRC Press, Boca Raton, FL, USA.

Kalinski, M.E. (1998). Determination of in situ v_s and g_{max} using surface wave measurements in cased and uncased boreholes. PhD Thesis, Department of Civil Engineering, University of Texas at Austin, Austin, Texas.

Kalinski, M.E., and Stokoe, K.H. (1998). Stress wave measurements in open holes in soil. Final Rep., Department of Civil Engineering, University of Texas at Austin, Austin, Texas.

Kalinski, M.E., Stokoe, K.H., O'Neill, M.W. (2001). Use of SASW measurements to evaluate the effect of line slurry conditioning in drilled shafts. *Journal of Environmental & Engineering Geophysics*, 6(4):147-156.

Konder, R.L. (1963). Hyperbolic stress strain response: cohesive soils. Journal of the Soil Mechanics and Foundations Division: *Proceedings of the American Society of Civil Engineers,* 89(1): 115-144.

Kraft, L.M., Ray, R.P. and Kagawa, T. (1981). Theoretical *t-z* Curves. *Journal of the Geotechnical Engineering Division, ASCE* 107(11): 1543-1561.

Mylonakis, G. (1995). Contributions to Static and Seismic Analysis of Piles and Pile-Supported Bridge Piers. PhD Thesis, State University of New York at Buffalo, New York, NY.

Mylonakis, G. (2001). Winkler Modulus for Axially Loaded Piles. *Géotechnique* 51(5): 455-461.

Mylonakis, G. and Gazetas, G. (1998). Settlement and additional internal forces of grouped piles in layered soil. *Géotechnique* 48(1): 55-72.

O'Neill, M.W. (2001). Side resistance in piles and drilled shafts. *Journal of Geotechnical and Geoenvironmental Engineering*, *ASCE* 127(1): 1-16.

Ottaviani, M. (1975). Three-dimensional finite element analysis of vertically loaded pile groups. *Géotechnique* 25(2): 159-174.

Poulos, H.G. and Davis, E.H. (1968). The settlement behaviour of single axially loaded incompressible piles and piers. *Géotechnique* 18: 351-371.

Poulos, H.G., and Davis, E.H. (1980). Pile foundation analysis and design. Wiley. New York, NY, 397 p.

Randolph, M.F. and Wroth, C.P. (1978). Analysis of deformation of vertically loaded piles. *Journal of the Geotechnical Engineering Division, ASCE* 104(12): 1465-1488.

Randolph, M.F., Cater, J.P. and Wroth, C.P. (1979). Driven piles in clay – the effects of installation and subsequent consolidation. *Géotechnique* 29(4): 361-393.

Scott, R.F. (1981). Foundation analysis, 1st edition. Prentice-Hall, Englewood Cliffs, NJ, USA.

Seed, H.B. and Reese, L.C. (1957). The action of soft clay along friction piles. Transactions, *ASCE* 122: 731-754.

Skempton, A.W. (1959). Cast in-situ bored piles in London clay. *Géotechnique* 9(4):153-173.

Syngros, K. (2004). Seismic response of piles and pile-supported bridge piers evaluated through case histories. PhD Thesis, the City College of the City University of New York, New York, NY, USA.

Vardanega, P.J. and Bolton, M.D. (2011a). Predicting the shear strength mobilization of London clay. Proceedings of the 15th European Conference on Soil Mechanics and Geotechnical Engineering: geotechnics of hard soils – weak rocks (eds A. Anagnostopoulos, M. Pachakis and C. Tsatsanifos), Amsterdam, the Netherlands, IOS Press BV. vol. 1: 487-492.

Vardanega, P.J. and Bolton, M.D. (2011b). Strength mobilization in clays and silts. *Canadian Geotechnical Journal,* 48(10): 1485-1503.

Vardanega, P.J., Williamson, M.G. and Bolton, M.D. (2012). Bored pile design in stiff clay II: mechanisms and uncertainty. *Proceedings of the Institute of Civil Engineers – Geotechnical Engineering* 165(4): 233-246, corrigendum 166(5): 518.

Vardanega, P.J. (2015). Sensitivity of simplified pile settlement calculations to parameter variation in stiff clay. In Proceedings of the XVI ECSMGE. ICE Publishing London, UK, 7: 3777-3782.

Vijayvergiya, V.N. (1977). Load movement characteristics of piles. *Proceedings of Ports'77: the 4th annual symposium of the Waterway, Port, Coastal and Ocean Division of ASCE*, ASCE, New York: 269-284.

DFI Journal Underwriters